Substituent effects on H_3^+ formation via H_2 roaming mechanisms from organic molecules under strong-field photodissociation (F)

Nagitha Ekanayake (iD), Muath Nairat, Nicholas P. Weingartz, Matthew J. Michie (iD), Benjamin G. Levine (iD), and Marcos Dantus (iD)

COLLECTIONS

(F)   This paper was selected as Featured

View Online   **Export Citation**   **CrossMark**

ARTICLES YOU MAY BE INTERESTED IN

An efficient approximate algorithm for nonadiabatic molecular dynamics
The Journal of Chemical Physics **149**, 244117 (2018); https://doi.org/10.1063/1.5046757

HOD on Ni(111): Ab Initio molecular dynamics prediction of molecular beam experiments
The Journal of Chemical Physics **149**, 244706 (2018); https://doi.org/10.1063/1.5059357

Electronic spectroscopy of methyl vinyl ketone oxide: A four-carbon unsaturated Criegee intermediate from isoprene ozonolysis
The Journal of Chemical Physics **149**, 244309 (2018); https://doi.org/10.1063/1.5064716

149, 244310

Substituent effects on H₃⁺ formation via H₂ roaming mechanisms from organic molecules under strong-field photodissociation

Nagitha Ekanayake,[1] Muath Nairat,[1] Nicholas P. Weingartz,[1] Matthew J. Michie,[1] Benjamin G. Levine,[1] and Marcos Dantus[1,2,a)]
[1]*Department of Chemistry, Michigan State University, East Lansing, Michigan 48824, USA*
[2]*Department of Physics and Astronomy, Michigan State University, East Lansing, Michigan 48824, USA*

Roaming chemical reactions are often associated with neutral molecules. The recent findings of roaming processes in ionic species, in particular, ones that lead to the formation of H_3^+ under strong-field laser excitation, are of considerable interest. Given that such gas-phase reactions are initiated by double ionization and subsequently facilitated through deprotonation, we investigate the strong-field photodissociation of ethanethiol, also known as ethyl mercaptan, and compare it to results from ethanol. Contrary to expectations, the H_3^+ yield was found to be an order of magnitude lower for ethanethiol at certain laser field intensities, despite its lower ionization energy and higher acidity compared to ethanol. In-depth analysis of the femtosecond time-resolved experimental findings, supported by *ab initio* quantum mechanical calculations, provides key information regarding the roaming mechanisms related to H_3^+ formation. Results of this study on the dynamics of dissociative half-collisions involving H_3^+, a vital cation which acts as a Brønsted–Lowry acid protonating interstellar organic compounds, may also provide valuable information regarding the formation mechanisms and observed natural abundances of complex organic molecules in interstellar media and planetary atmospheres. *Published by AIP Publishing.* https://doi.org/10.1063/1.5065387

INTRODUCTION

Since the first interpretation by Townsend *et al.* in formaldehyde decomposition,[1] roaming chemical reactions have been intensively studied in unimolecular decomposition and isomerization reactions involving highly excited polyatomic molecules as evidenced by recent reviews.[2–7] Roaming reactions bypass the conventional transition-state in the reaction coordinate and proceed through trajectories that may be far from the minimum energy pathway. The roaming species explores relatively flat regions of the potential energy surface before it completes the reaction. This results in unexpected products with unexpected product state distributions. While roaming is widely studied in unimolecular reactions in the gas phase, roaming mechanisms in bimolecular reactions[8–10] as well as in the liquid phase reactions[11] are now gaining considerable attention. However, the better known roaming reactions involve decomposition or isomerization of excited state neutral molecules. There are only a small number of studies on unimolecular dissociation of polyatomic ions involving roaming, referred to as ionic roaming. A theoretical investigation by Mebel and Bandrauk predicted the involvement of H_2 roaming in the dissociative ionization of allene.[12] In our recent studies involving time-resolved and coincidence measurements on the strong-field double-ionization of small alcohols, we provided the first systematic experiment and theoretical evidence that H_3^+ ions are formed through a roaming mechanism involving H_2 molecules.[13,14] Unlike roaming reactions occurring

near the dissociative threshold in predissociative states, ionic roaming mechanisms do not seem to require near threshold excitation.

In the case of methanol, the neutral hydrogen molecule produced by the parent dication roams around the $HCOH^{2+}$ dication until it abstracts a proton to form H_3^+, thus acting as a Brønsted–Lowry base. Our findings revealed that H_3^+ formation occurs within 100 fs or 250 fs depending on the pathway.[13] Inspired by these novel findings, we continued our investigation by examining the effect of length of the primary carbon chain of small alcohol molecules on the formation of the H_3^+ molecular ion.[14] We expected that increasing the number of H atoms in the molecule would enhance the H_3^+ yield. The experimental findings, confirmed by *ab initio* molecular dynamics simulations, showed that the yield of H_3^+ decreases as the chain length increases. Furthermore, in that study, we found evidence for the existence of additional H_3^+ formation mechanisms involving hydrogen migration for small alcohols.

Both aforementioned studies, as well as a several other studies[15–17] on H_3^+ formation from organic molecules under strong laser fields, were focused on alcohols. In this study, we explore how the functional group affects the yield of H_3^+. It is conceivable that certain classes of compounds may be more or less likely to produce H_3^+. For this reason, functional-group specific investigations are important. Our overall goal is to determine the key molecular properties that determine H_2 formation and the subsequent formation of H_3^+. These findings will lead to a better understanding of these sparsely known roaming reactions occurring in ionic species.

---

a)Author to whom correspondence should be addressed: dantus@chemistry.msu.edu

Here, we examine and report results for ethanethiol isotopologues, particularly looking at the substituent effects on the roaming molecular hydrogen mechanism and subsequent H_3^+ formation when the hydroxyl (–OH) functional group is replaced by a thiol (–SH) group. The choice is partly motivated by the following reasons. Previously published studies have extensively elaborated that H_3^+ production from small alcohols under strong-field laser conditions at 10^{14} W/cm^2 is primarily initiated by double ionization of the parent.[13–17] Given that thiols have a slightly lower second ionization potential compared to their alcohol equivalent (by 2.7 eV), the cross section for producing the doubly ionized reaction precursor via femtosecond excitation is expected to be higher. Furthermore, in our previous work with ethanol, we provided extensive evidence that the primary pathway producing H_3^+ involves deprotonation of hydroxyl proton by the roaming H_2. It is well-known that thiols (pKa $\approx$ 11) are more acidic than alcohols (pKa $\approx$ 16). For example, the deprotonation energy for ethanethiol is 1488 kJ/mol, while that of ethanol is 1587 kJ/mol.[18] Thus, compared to alcohols, in the process of producing H_3^+, it is easier to deprotonate the thiol. Therefore, it is intuitive to expect an overall higher H_3^+ production from a thiol molecule compared to its alcohol counterpart. Hence, here we experimentally and theoretically investigated the H_3^+ production from ethanol (CH_3CH_2OH) and ethanethiol (CH_3CH_2SH) via strong-field laser ionization. H_2D^+ production from partially deuterated species, CH_3CH_2OD and CH_3CH_2SD, was also compared with their natural counterparts to confirm the observations and to investigate any isotopic substitution effects. The photodissociation of ethanethiol in the UV region (214–254 nm) producing neutral fragments has been reported.[19,20] However, to the best of our knowledge, we present here the first quantitative study of H_2 roaming and H_3^+ formation from sulfur-containing compounds as well as characterizing substituent effects on H_3^+ formation in any wavelength regime.

In interstellar chemistry, H_3^+ is considered to be the most important molecular ion because it is responsible for the formation of water molecules as well as an abundance of organic molecules.[21] Behaving as a Brønsted–Lowry acid,[22,23] H_3^+ protonates interstellar atoms, molecules, and ions leading to the creation of complex organic molecules, which may be partly responsible for life in the universe.[24,25] A fundamental understanding regarding the dynamics and mechanisms of reactive collisions involving H_3^+ can be obtained from laser-induced photodissociation processes producing H_3^+, which can be considered the reverse "half collision" of the full reaction profile.[26,27] It is shown that interstellar organosulfur compounds play an important role in maintaining the atmospheric sulfur cycle.[28,29] In interstellar ice, organosulfur compounds such as carbonyl sulfide (OCS) are found to exist with a relative abundance about 2% compared to water ice.[30] Therefore, a detailed investigation of the photodissociation dynamics leading to the formation of H_3^+ in sulfur-containing compounds not only provides valuable information regarding the formation mechanisms but also may contribute to a better understanding of reaction mechanisms prevalent in atmospheric sulfur chemistry.

METHODS

Experimental—Mass spectrometry

In order to qualitatively and quantitatively identify the H_3^+ formation trends from the two organic compounds under investigation, we examined the total H_3^+ yield (i.e., the integral over the H_3^+ peak) as well as the fractional H_3^+ production, which is defined as the ratio between the total H_3^+ yield and the sum of all ions originating from the parent molecular ion. In our previous work, an in-depth analysis performed through time-of-flight (TOF) measurements and photoion-photoion coincidence measurements confirmed that the above two parameters, i.e., the total H_3^+ yield and the fractional H_3^+ production, satisfactorily quantify the formation trends between different molecules, given that the measurements were made under careful control of experimental conditions and the single- and double-ionization cross sections (which strongly depend on corresponding ionization potentials) do not vary significantly between the molecules under analysis.[14] In that study, we explicitly showed that the above analysis methods are valid even when comparing H_3^+ production from molecules such as menthol and 1-propanol, in which the second ionization potentials differ by approximately 3.9 eV. In regards to this work, the single ionization potential for ethanol and ethanethiol is 10.5 eV and 9.3 eV, respectively.[18] The calculated second ionization energies are 30.1 eV for ethanol and 27.4 eV for ethanethiol, as obtained at the CR-CC(2,3)/cc-pVQZ level of theory. Thus, the difference in second ionization energies between two species is 2.7 eV and justifies the applicability of our previous analysis method for this particular study.

The laser system, experimental apparatus, and data acquisition methods used in this study are described in detail elsewhere.[13,14] Briefly, a 40-fs 800-nm pulse causes dissociative ionization of ethanol or ethanethiol, and the generated ions were analyzed using a time-of-flight (TOF) mass spectrometer with a measurement uncertainty of less than 5%. All intensity-dependent measurements were carried out in a linearly polarized laser field with the polarization axis parallel to the time-of-flight axis. For transient measurements, a Mach–Zehnder interferometer was used to split the laser beam into pump and probe pulses in order to obtain formation time scales via femtosecond time-resolved mass spectrometry. The pump intensity was kept at 2.0×10^{14} W/cm^2. The probe intensity was set to 0.75×10^{14} W/cm^2 such that the precursor ion for H_3^+ formation created by the intense pump pulse, i.e., the parent dication, is disrupted by the weak probe. The laser intensity was calibrated by measuring Ar^{2+}/Ar^+ and N_2^{2+}/N_2^+ yield ratios[31,32] and confirmed against the calculated intensity based on optical measurements within a factor of 2. Further details regarding the intensity calibration can be found in Sec. (a) of the supplementary material. High-purity liquid samples were thoroughly dehydrated using 4-Åmolecular sieve desiccants. Prior to the introduction to the interaction region, all liquid samples were outgassed using several iterations of freeze-pump-thaw to minimize possible contributions to the mass spectra from atmospheric contaminants. The base pressure of the vacuum region of the mass spectrometer was kept at less than 1×10^{-9} Torr and all the measurements were made at a sample gas pressure of $1.0 \pm 0.5 \times 10^{-6}$ Torr, at room

temperature. All measured ion yields were corrected taking into account the Bayard–Alpert ion gauge's sensitivity for the specific gas sample being measured.

In all mass spectra obtained, contributions from C^{4+} (quadruply ionized carbon) with an $m/z = 3$ were insignificant as confirmed by the lack of ions at $m/z = 4$, corresponding to C^{3+} (an essential precursor for formation of C^{4+}), under our experimental conditions. In addition, when studying deuterated isotopologues, H_3^+ yield became indistinguishable from HD^+ yield due to their degeneracy in the mass spectrum at $m/z = 3$. Therefore, we only analyzed data for H_2D^+ yields from CH_3CH_2OD and CH_3CH_2SD.

Computational—*Ab initio* quantum mechanical calculations

The optimized ground state structures of ethanol and ethanethiol were calculated using coupled cluster singles and doubles (CCSD) while employing the cc-pVQZ basis set. Single point calculations incorporate a further noniterative triples correction through CR-CC(2,3), using the same basis set for the neutral and doubly charged electronic configurations. Global and local minima for doubly charged ethanol and ethanethiol were calculated at the CCSD/aug-cc-pVDZ level of theory. At the neutral structure minima of ethanol and ethanethiol, Mulliken population analyses were performed

for neutral and doubly charged electronic configuration at the equation-of-motion (EOM)-CCSD/cc-pVQZ level of theory. This allows us to estimate the change in the electron density upon instantaneous double ionization prior to any nuclear rearrangements. All CCSD geometry optimizations were carried out using the Molpro 2012.1[33–35] software package, while CR-CC(2,3) and EOM-CCSD parts were calculated using General Atomic and Molecular Electronic Structure System (GAMESS).[36–38]

RESULTS AND DISCUSSION

Experimental H_3^+ yields

We begin our study by comparing the H_3^+ production from the two molecular species under investigation. The complete time-of-flight mass spectra for CH_3CH_2OH and CH_3CH_2SH are given in Fig. 1. Figure 2 summarizes the measured intensity-dependent H_3^+ yields from ethanol and ethanethiol photodissociation by a linearly polarized laser field with a peak intensity ranging from 1.5×10^{14} to 3.5×10^{14} W/cm^2. Since all acquisitions were made under comparable experimental conditions, several key comparisons can be made from the data obtained. When comparing the integrated ion yields from CH_3CH_2OH and CH_3CH_2SH [Fig. 2(a)], it is evident that H_3^+ production from CH_3CH_2OH is about 3–4 times higher
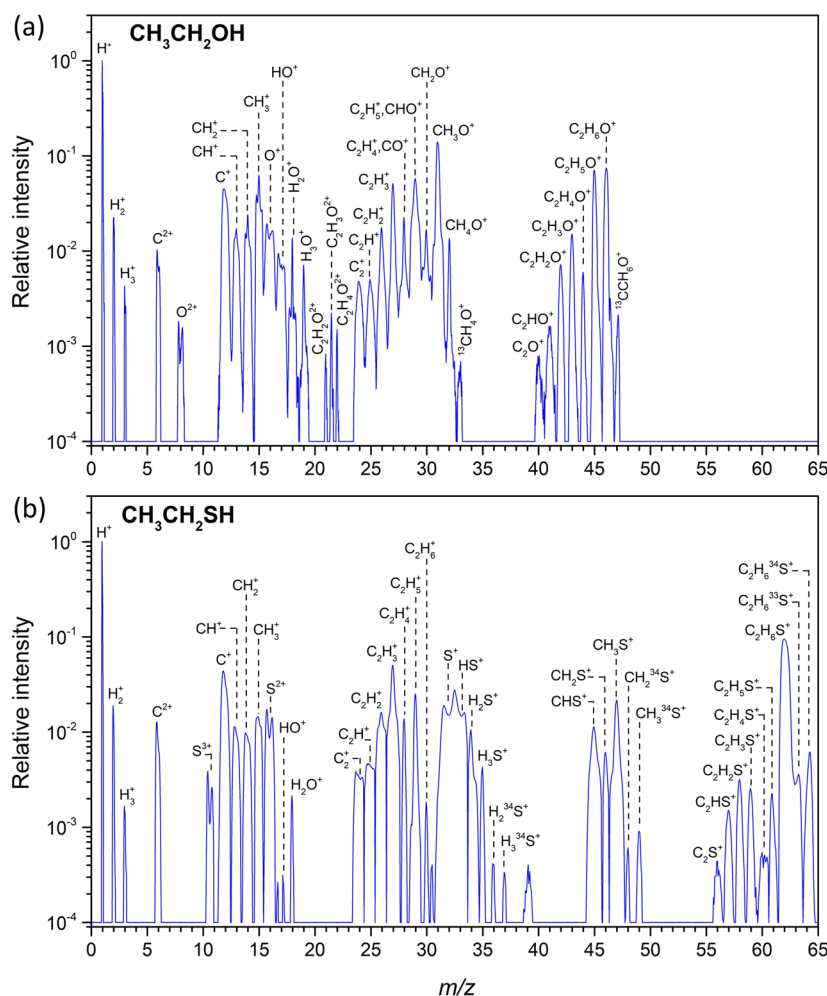

FIG. 1. The time-of-flight mass spectrum for the dissociative ionization of (a) CH_3CH_2OH and (b) CH_3CH_2SH in a linearly polarized laser focus of 2×10^{14} W/cm^2.
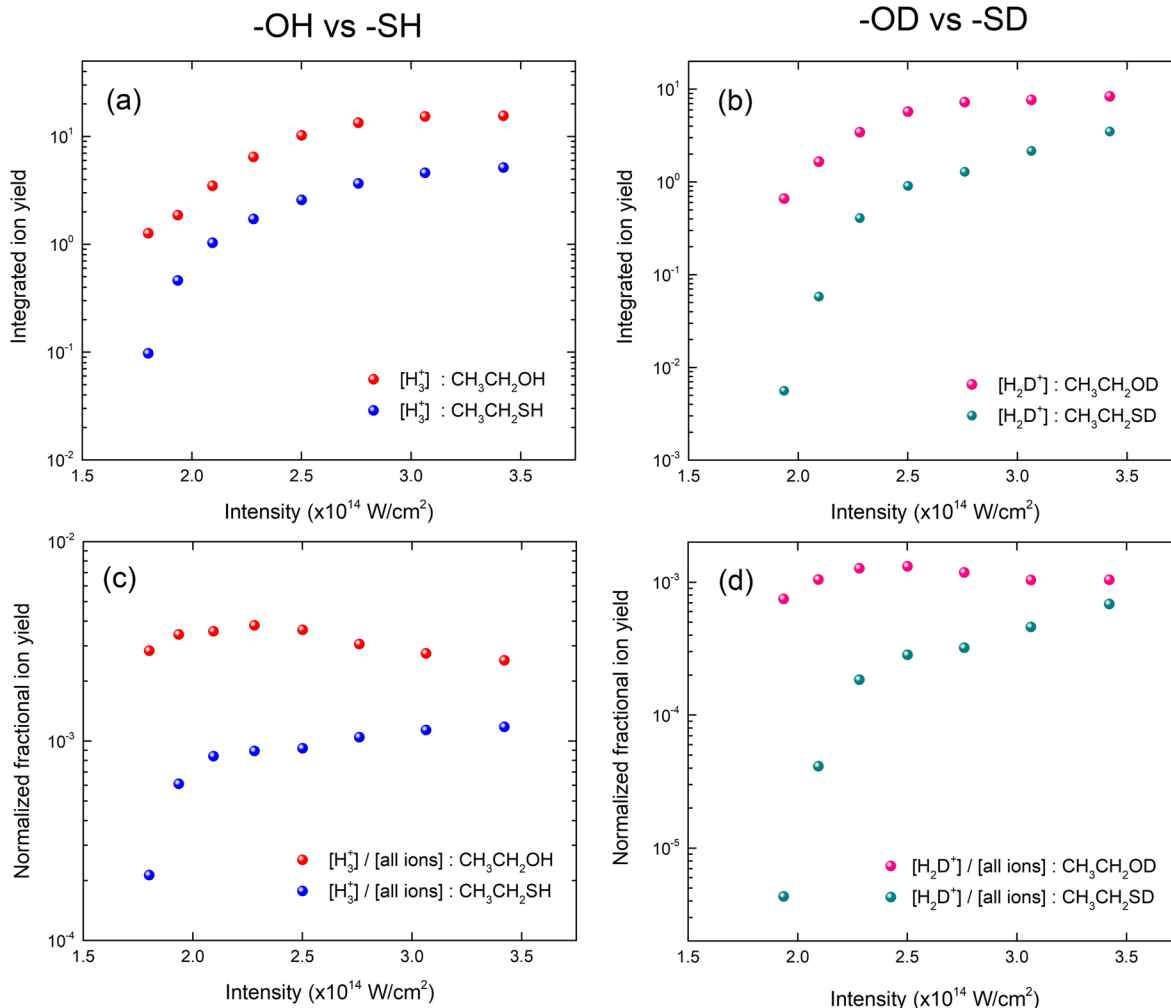
FIG. 2. Experimental photodissociation yields for (a) CH_3CH_2OH, (b) CH_3CH_2SH, (c) CH_3CH_2OD, and (d) CH_3CH_2SD ionized by an 800-nm radiation field with a 40-fs pulse duration. Data shown in (a) and (b) have a combined error (both systematic and statistical) of ±5% on the y scale, where the calculated error (obtained through propagation of error) on the y scale of data shown in (c) and (d) is ±7%. As detailed in the experimental section, the intensity calibration is accurate within a factor of 2.

compared to that of CH_3CH_2SH for peak intensities greater than 2×10^{14} W/cm^2. The difference is much greater, over an order of magnitude, as the intensity is decreased towards the detection threshold. Qualitatively, a similar trend can be observed between CH_3CH_2OD and CH_3CH_2SD [Fig. 2(b)] in the production of H_2D^+.

A closer look at the data reveals that the integrated H_3^+ yields from CH_3CH_2OH and CH_3CH_2SH are slightly higher than the H_2D^+ yields produced from CH_3CH_2OD and CH_3CH_2SD. In the former case, i.e., for non-deuterated species, each integrated H_3^+ yield may contain contributions from up to six possible H_3^+ formation pathways. In contrast, in the latter case, the H_2D^+ production is limited to only three pathways, at most. However, one of these three possible pathways, the pathway that produces the cation from two α-hydrogens combining with the proton from the terminal functional group, is the dominant channel providing the highest contribution to the cation yield.[14] Therefore, it is expected that the overall H_3^+ production from six pathways is slightly higher compared to H_2D^+ production under the experimental conditions employed here.

When expressed as a fractional yield, the H_3^+ production from CH_3CH_2OH and CH_3CH_2SH [Fig. 2(c)] as well as H_2D^+ from CH_3CH_2OD and CH_3CH_2SD [Fig. 2(d)] qualitatively follow a similar trend as observed with the corresponding integrated H_3^+ yields. Based on the differential ion yield analysis (see the subsequent text), we observed that both H_3^+ from CH_3CH_2OH and H_2D^+ from CH_3CH_2OD reach a saturation at an earlier peak intensity ($\sim 2.5 \times 10^{14}$ W/cm^2) compared to H_3^+ from CH_3CH_2SH and H_2D^+ from CH_3CH_2SD (above 2.75×10^{14} W/cm^2). Interestingly, these features manifest in fractional yield measurements as H_3^+ yields from CH_3CH_2OH and H_2D^+ from CH_3CH_2OD do not vary much across the range of intensity being measured, while CH_3CH_2SH and CH_3CH_2SD data indicate a significant variation across the same intensity range. Also, this close resemblance in yields obtained from deuterated and non-deuterated species indicated that in both ethanol and ethanethiol, H_3^+ formation is primarily dominated by the mechanisms which involve the roaming H_2 generated from carbon-bound hydrogens deprotonating the terminal functional group.

Because the double ionization process depends nonlinearly on the peak intensity, it is important to consider the Gaussian intensity distribution of the laser focus. Therefore, at some given total laser pulse energy, the peak intensity near the center of the beam is significantly higher than at a larger radial distance. The integration over multiple different intensities is know as the "volume effect" and it can mask the threshold of intensity dependent effects. In order to investigate the total ion production from a given intensity bin, we used a differential analysis method.[39] The differential ion yield (D_I) evaluated at a given ion intensity I is represented by

$$D_I = [i^+]_I - [i^+]_{0.85I}, \qquad (1)$$

where $[i^+]_I$ is the integrated ion yield measured at a peak intensity of I and $[i^+]_{0.85I}$ is that measured at a peak intensity of $0.85I$. Figure 3 indicates the evaluated differential ion yields for H_3^+ and H_2D^+ formation from ethanol and ethanethiol together with the variation of the corresponding molecular cation. The differential yield measurements may carry a certain amount of noise resulting from the subtraction; however, they clearly reveal that first ionization does occur at an earlier peak intensity for ethanethiol and that double ionization occurs at the expense of single ionization. Furthermore, it is

evident that the yield of H_3^+ does not occur at lower intensities as naively expected from the lower double ionization energy for ethanethiol. In fact, the maximum H_3^+ yield for ethanethiol occurs at a relatively higher laser peak intensity than for ethanol. Even though the yield for ethanethiol cation is always higher, the resulting yield of H_3^+ is always lower compared to ethanol.

Ab initio quantum chemical calculations

The reduction in observed H_3^+ yield from ethanethiol relative to ethanol can be understood by exploring results from *ab initio* electronic structure calculations. In our previous work,[14] we showed that a major influence on the H_3^+ production stems from the original ground state geometry and its ability to produce an H_2 molecule upon double ionization in the vicinity of a third proton that can be abstracted during the course of the roaming reaction. When H_3^+ is formed from alcohols, there are two primary intramolecular structural changes that take place which lead to the formation of a H_2 molecule and eventually H_3^+. They are the elongation of C–H bonds and the narrowing of the H–C–H angle on the α-carbon atom, characterized by the shortening of the H–H distance between the two α-hydrogens.[14]
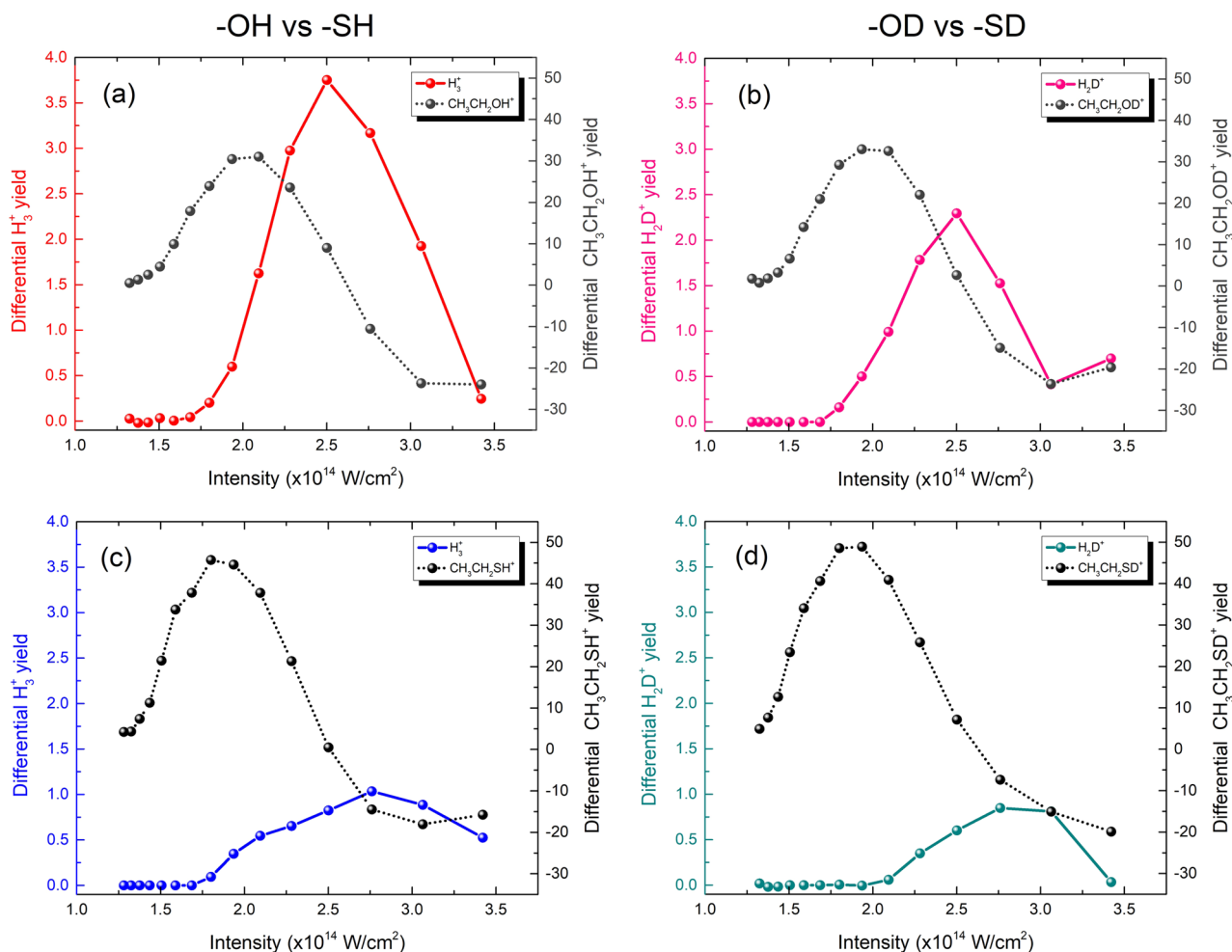

FIG. 3. Calculated differential ion yields for (a) CH_3CH_2OH, (b) CH_3CH_2OD, (c) CH_3CH_2SH, and (d) CH_3CH_2SD ionized by an 800-nm radiation field with a 40-fs pulse duration. Data shown have a combined error of ±5% on the y scale. As detailed in the experimental section, the intensity calibration is accurate within a factor of 2.

These structural changes are initiated by intramolecular atomic charge redistribution, which occurs immediately following double ionization by an intense femtosecond laser pulse. Here, we evaluated the density matrix and Mulliken population analysis at the neutral ground state global minima of both molecules [*anti*-configuration for ethanol and ethanethiol in *gauche*-configuration as obtained using CR-CC(2,3)/cc-pVQZ//CCSD/cc-pVQZ; see the supplementary material, Sec. (b) for detailed information regarding *ab initio* calculations] at the EOM-CCSD/cc-pVQZ//CCSD/cc-pVQZ level of theory. This has been implemented using neutral and doubly charged electronic configurations to compare any changes in the electronic density when the laser field doubly ionizes the neutral molecule instantaneously prior to any nuclear rearrangements. The obtained atomic charges are summarized in Fig. 4.

In ethanol, the electron density depletion on oxygen due to the removal of a lone electron pair by an intense femtosecond pulse is partially compensated by the electronic induction from the α-carbon and the α-hydrogen atoms [Fig. 4(a)]. Such a decrease in electron density on α-hydrogens, as characterized by 0.33 charge units increase in atomic charge (from 0.03 charge units to 0.36 charge units), weakens the αC–H bonds, causing bonds to elongate and closing of the H–αC–H angle. Consequently, the H–H distance between the two α-hydrogens shortens, resulting in H_2 detachment and roaming. However, in the case of ethanethiol, the electronic depletion on the sulfur atom is less—as sulfur has 8 more electrons in the neighboring outer shell compared to oxygen. Therefore, electron induction from the α-carbon and α-hydrogens is less significant [Fig. 4(b)]. For example, here the average increase in atomic charge on α-hydrogens is only about 0.16

charge units; 50% less than the increase on α-hydrogens in ethanol. This reduces the weakening of the αC–H bonds and the narrowing of the H–αC–H angle in ethanethiol. Consequently, the H–H distance between the two α-hydrogens does not reduce as much compared to ethanol. Thus, the formation of H_2 and subsequent production of H_3^+ from ethanethiol would be expected to be lower. In addition, we notice that compared to β-hydrogens, α-hydrogens are the ones that are most prone to decrease in electron density upon double ionization. In ethanol for instance, the atomic charge on α-hydrogens increases by 0.33 charge units, while on β-hydrogens it only increases by 0.13–0.21 charge units. This results in less structural deformation on the terminal methyl site, thus impeding favorable conditions for β-hydrogen detachment. Therefore, we anticipate a low H_3^+ yield from hydrogen atoms involving the terminal methyl site in both molecules. This is in agreement with our previously published results on ethanol.[14]

Figure 5 summarizes a comparison between the neutral and doubly charged minima of ethanol and ethanethiol optimized at the CCSD/aug-cc-pVDZ level of theory. It is important to note that these doubly charged minima are not necessarily global minima; however, they represent an important point of interest that is reachable from the neutral structure minima upon instantaneous double ionization (see the supplementary material, Sec. (b) for detailed information). In ethanol, compared to the stable ground state, the doubly charged structure subsequent to atomic charge redistribution (discussed above) indicates a 0.56 Å elongation of the αC–H bond length and a substantial reduction in the H–αC–H bond angle [Fig. 5(a)]. These rearrangements shorten the distance between the two α-hydrogens by 0.95 Å, causing
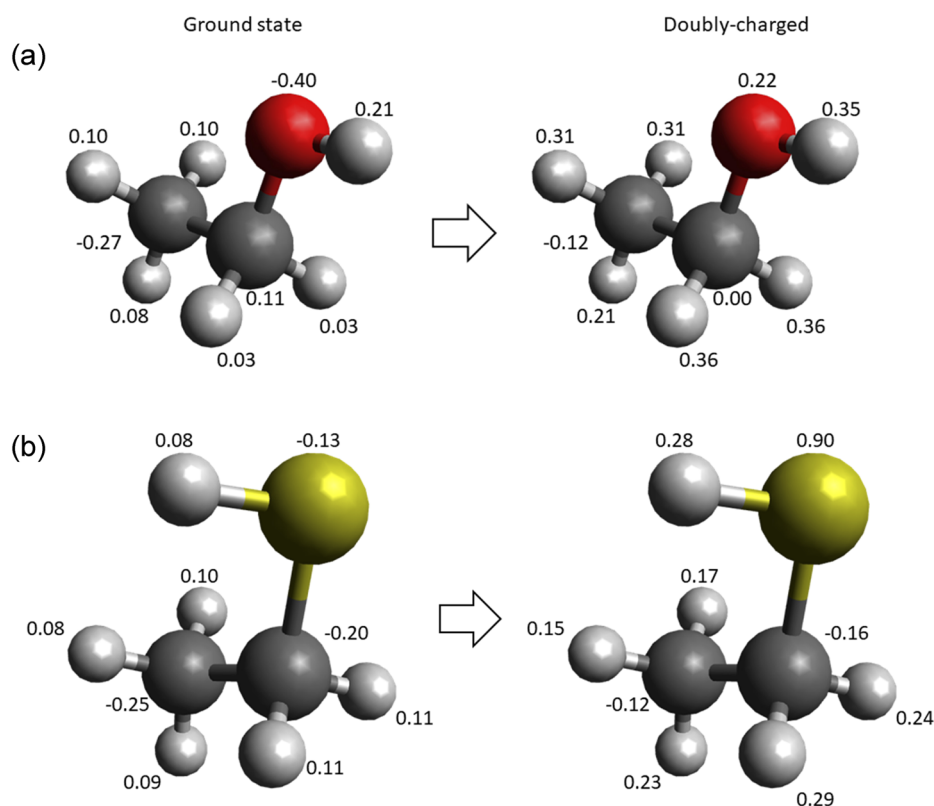

FIG. 4. Atomic charges obtained from Mulliken population analysis at the EOM-CCSD/cc-pVQZ level of theory for neutral and doubly charged electronic configurations of (a) ethanol and (b) ethanethiol global structures minima as obtained using CCSD/cc-pVQZ.
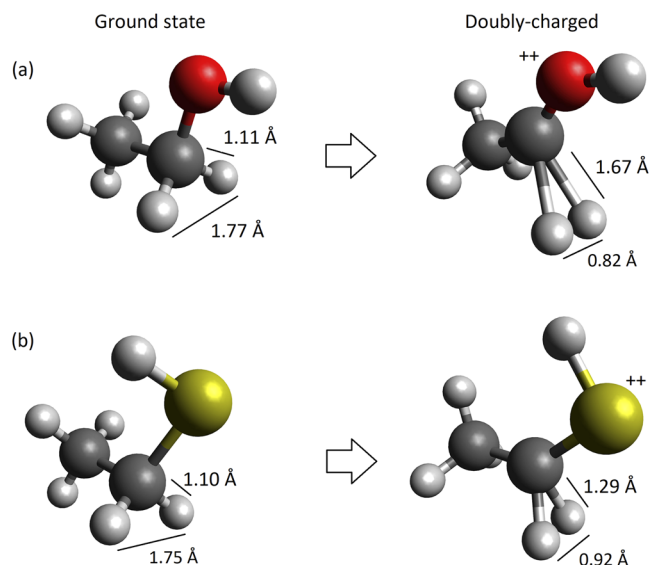
FIG. 5. Neutral and doubly charged structure minima of (a) ethanol and (b) ethanethiol carried out at the CCSD/aug-cc-pVDZ level of theory. Bond length of the αC–H bonds and H–H distance between the two α-hydrogens, which are involved in the roaming H_2 formation mechanism leading to the formation of H_3^+, are shown. Doubly charged ethanol shows longer αC–H bonds and shorter H–H distance allowing H_2 ejection to be more efficient.
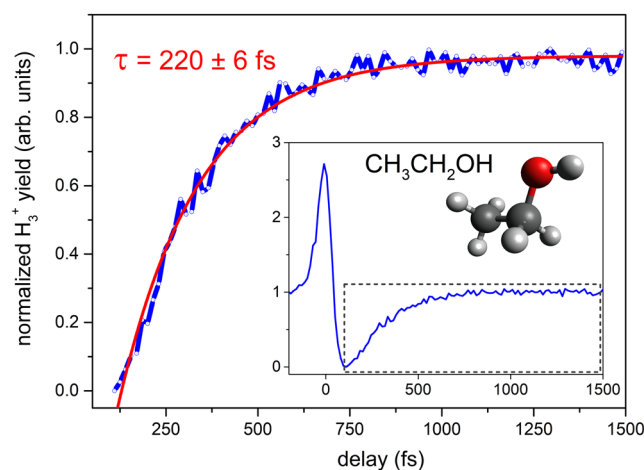

FIG. 6. Normalized H_3^+ yield (blue solid line) together with an exponential fit (red solid line) from dissociative ionization of CH_3CH_2OH as a function of applied time delay between pump and probe pulses. In the inset, the complete view of the normalized transient is shown where the dashed rectangle highlights the area of interest displayed in the main figure. Normalization was performed such that the minimum valve of the yield is 0 and the yield at large positive time delays ($\geq$750 fs) is 1.

the H–H distance to be 0.82 Å. In contrast, such key structural deformations are less pronounced when comparing the ethanethiol ground state structure to its doubly charged counterpart [Fig. 5(b)]. This results in the H–H distance only to be 0.92 Å for the two α-hydrogens. Therefore, H_2 detachment is less likely, resulting in a reduced yield of H_3^+ from ethanethiol. In doubly charged ethanol, when H_2 is formed, the hydroxyl hydrogen is in the *anti*-configuration, which is in close vicinity to the roaming H_2 molecule and facilitates H_3^+ formation. In contrast, when H_2 is formed from doubly charged ethanethiol, the thiol hydrogen is in the *eclipsed*-configuration, resulting in lower H_3^+ yield in ethanethiol relative to ethanol. This observation is also important as we proceed to understand the differences in formation time scales of H_3^+ from two molecules in the H_3^+ formation time scales section.

H_3^+ formation time scales

We carried out femtosecond pump-probe transient experiments on ethanol and ethanethiol. Similar to our previous studies, this technique makes use of a strong pump pulse to generate the doubly charged parent ion, the reaction precursor, and a weak probe pulse to intercept the formation of H_3^+. Further details on the technique, interpretation of the transient's features, and the method of extraction of the formation time are fully described in our previous studies.[13,14,40,41] Figure 6 displays the measured transient for ethanol together with the exponential fit [given by $y = y_0 + A(1 - exp(-t/\tau))$, where A is the amplitude, y_0 is the offset, and τ is the time constant] used to obtain the formation time and Fig. 7 shows those for ethanethiol.

Ethanol exhibits a formation time of 220 ± 6 fs, and an ~66% slower formation time is observed for ethanethiol with 365 ± 10 fs (see Fig. 7). In both cases, we maintain a 95%

confidence level for the fit parameters. The value obtained for ethanol is in good agreement with our previous[14] experimental findings (235 ± 10) as well as *ab initio* calculations (110–220 fs). As we confirmed previously,[14] in alcohols with long carbon chains (e.g., ethanol and 1-propanol), the roaming H_2 molecule primarily forms from the α-hydrogens and then abstracts the third hydrogen from the neighboring hydroxyl group in the formation of H_3^+. The H_3^+ yield involving exclusively H atoms from the terminal CH_3 group is insignificant compared to the other pathways.[14] Given the similarities in the molecular structures, we assume that the above conclusion remains valid for ethanethiol as well.

The prolonged formation time for ethanethiol can be qualitatively understood by turning our attention to the ground state and doubly charged molecular structures shown in Fig. 5. In the case of ethanol [see Fig. 5(a)], the two α-hydrogen atoms
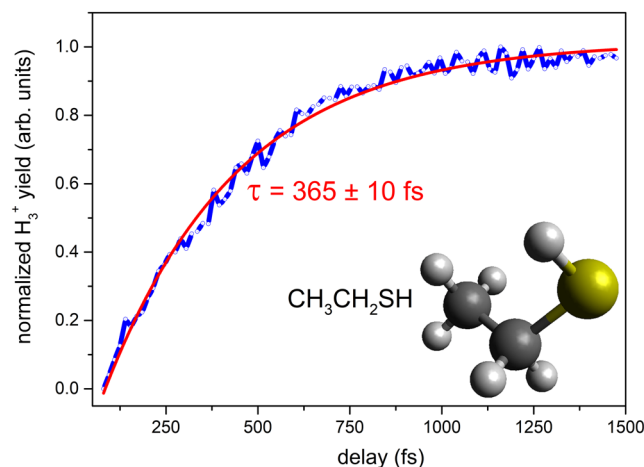

FIG. 7. Normalized H_3^+ transients from dissociative ionization of CH_3CH_2SH as a function of applied pump-probe delay. Normalization was performed as described in the caption of Fig. 6. Corresponding exponential fit is shown by the red solid line.

which are expected to detach and form the neutral H_2 molecule are in *anti*-conformation with respect to the hydrogen atom of the hydroxyl group, thus making it a shorter roaming distance and thus reaction time. However, in the case of ethanethiol [see Fig. 5(b)], the hydroxyl proton is in an *eclipsed* conformation relative to the two α-hydrogen atoms. This makes the H_2 roaming distance and/or SH rotation time much longer for ethanethiol, hence the H_3^+ formation time.

CONCLUSIONS

In this paper, we explored the effect of functional group substitution on the production of H_3^+ upon dissociative ionization in a strong laser field. We presented experimental results regarding the yields as well as the formation time scales for ethanethiol and compared them with those of ethanol. Theoretical results were obtained to explore structural differences in both the ground and doubly ionized states. Our findings reveal that atomic substitution can cause a substantial change in both the yield and time scale in the production of H_3^+ from organic molecules, which proceeds through a H_2 roaming mechanism initiated by the double ionization of the parent cation.

Due to the lower second ionization potential and deprotonation energy in ethanethiol compared to those of ethanol, we expected a higher H_3^+ production from ethanethiol. To our surprise, we observed the contrary. In fact, we found that H_3^+ formation is significantly lowered by a sulfur substitution in the functional group. Depending on the peak laser intensity, this suppression due to substitution can amount to an order of magnitude reduction in H_3^+ formation. In addition, the observed faster formation time for H_3^+ from ethanol compared to ethanethiol is consistent with the reduced yield. Reasons for why the yield is reduced and the formation time is extended are revealed by *ab initio* electronic structure calculations for both ground state and doubly charged structural configurations of the corresponding molecules. First, we found that the H_2 yield may be lower for thiols, given that doubly ionized sulfur is less electron withdrawing than doubly ionized oxygen. Thus, the C–H elongation and H–C–H bonding angle is not as amenable in the formation of neutral H_2 in thiols. Second, we found that for ethanol, the two α-hydrogen atoms are in anti-conformation with respect to the OH hydrogen atom, while for ethanethiol, the SH hydrogen atom is in eclipsed-conformation. This results in longer H_2 roaming due to distance or time for SH group rotation and hence longer H_3^+ formation time.

H_3^+ plays a vital role in the formation of complex organic molecules in interstellar space by initiating several distinct chains of ion-atom and ion-molecule chemical reactions.[21] The unimolecular reactions involving ethanethiol studied here exhibit an unfavorable condition for the formation of H_3^+; inversely, it can be deduced that reactive collisions involving H_3^+ in the interstellar space with an organosulfur compounds would be expected to have low probability for reversibility. The findings presented here regarding yield and time scales for the dissociative half-collision leading to H_3^+ production through H_2 roaming in ionic species may help in better understanding the observed natural abundance of organosulfur molecules in interstellar molecular clouds.

SUPPLEMENTARY MATERIAL

See supplementary material for additional information regarding laser intensity calibration and *ab initio* calculations.

[1]D. Townsend, Science **306**, 1158 (2004).

[2]J. M. Bowman and A. G. Suits, Phys. Today **64**(11), 33 (2011).

[3]J. M. Bowman and B. C. Shepler, Annu. Rev. Phys. Chem. **62**, 531 (2013).

[4]J. M. Bowman, Mol. Phys. **112**, 2516 (2014).

[5]S. Maeda, T. Taketsugu, K. Ohno, and K. Morokuma, J. Am. Chem. Soc. **137**, 3433 (2015).

[6]J. M. Bowman and P. L. Houston, Chem. Soc. Rev. **46**, 7615 (2017).

[7]X. Yang, D. C. Clary, and D. M. Neumark, Chem. Soc. Rev. **46**, 7481 (2017).

[8]B. Joalland, Y. Shi, A. Kamasah, A. G. Suits, and A. M. Mebel, Nat. Commun. **5**, 1 (2014).

[9]N. D. Coutinho, V. H. C. Silva, H. C. B. De Oliveira, A. J. Camargo, K. C. Mundim, and V. Aquilanti, J. Phys. Chem. Lett. **6**, 1553 (2015).

[10]F. A. L. Mauguière, P. Collins, S. Stamatiadis, A. Li, G. S. Ezra, S. C. Farantos, Z. C. Kramer, B. K. Carpenter, S. Wiggins, and H. Guo, J. Phys. Chem. A **120**, 5145 (2016).

[11]A. S. Mereshchenko, E. V. Butaeva, V. A. Borin, A. Eyzips, and A. N. Tarnovsky, Nat. Chem. **7**, 562 (2015).

[12]A. M. Mebel and A. D. Bandrauk, J. Chem. Phys. **129**, 224311 (2008).

[13]N. Ekanayake, M. Nairat, B. Kaderiya, P. Feizollah, B. Jochim, T. Severt, B. Berry, K. R. Pandiri, K. D. Carnes, S. Pathak, D. Rolles, A. Rudenko, I. Ben-Itzhak, C. A. Mancuso, B. S. Fales, J. E. Jackson, B. G. Levine, and M. Dantus, Sci. Rep. **7**, 4703 (2017).

[14]N. Ekanayake, T. Severt, M. Nairat, N. P. Weingartz, B. M. Farris, B. Kaderiya, P. Feizollah, B. Jochim, F. Ziaee, K. Borne, K. R. Pandiri, K. D. Carnes, D. Rolles, A. Rudenko, B. G. Levine, J. E. Jackson, I. Ben-Itzhak, and M. Dantus, Nat. Commun. **9**, 5186 (2018).

[15]Y. Furukawa, K. Hoshina, K. Yamanouchi, and H. Nakano, Chem. Phys. Lett. **414**, 117 (2005).

[16]N. Kotsina, S. Kaziannis, and C. Kosmidis, Int. J. Mass Spectrom. **380**, 34 (2015).

[17]T. Ando, A. Shimamoto, S. Miura, A. Iwasaki, K. Nakai, and K. Yamanouchi, Commun. Chem. **1**, 7 (2018).

[18]T. M. Ramond, G. E. Davico, R. L. Schwartz, and W. C. Lineberger, J. Chem. Phys. **112**, 1158 (2000).

[19]L. Bridges and J. M. White, J. Phys. Chem. **77**, 295 (1973).

[20]P. Svrčková, A. Pysanenko, J. Lengyel, P. Rubovič, J. Kočišek, V. Poterya, P. Slavíček, and M. Fárník, Phys. Chem. Chem. Phys. **17**, 25734 (2015).

[21]D. Smith and P. Španěl, Int. J. Mass Spectrom. Ion Process. **129**, 163 (1993).

[22]J. N. Brönsted, Recl. Trav. Chim. Pays-Bas **42**, 718 (1923).

[23]T. M. Lowry, J. Soc. Chem. Ind. **42**, 43 (1923).

[24]W. D. Watson, Rev. Mod. Phys. **48**, 513 (1976).

[25]A. Dalgarno and J. H. Black, Rep. Prog. Phys. **39**, 573 (1976).

[26]Y. B. Band and K. F. Freed, J. Chem. Phys. **63**, 3382 (1975).

[27]Y. B. Band, K. F. Freed, and D. J. Kouri, J. Chem. Phys. **74**, 4380 (1981).

[28]W. W. Kellogg, R. D. Cadle, E. R. Allen, A. L. Lazarus, and E. A. Martell, Science **175**, 587 (1972).

[29]P. Ehrenfreund and S. B. Charnley, Annu. Rev. Astron. Astrophys. **38**, 427 (2000).

[30]S. B. Charnley, S. D. Rodgers, and P. Ehrenfreund, Astron. Astrophys. **378**, 1024 (2001).

[31]C. Guo, M. Li, J. P. Nibarger, and G. N. Gibson, Phys. Rev. A **58**, R4271 (1998).

[32]T. Weber, M. Weckenbrock, A. Staudte, L. Spielberger, O. Jagutzki, V. Mergel, F. Afaneh, G. Urbasch, M. Vollmer, H. Giessen, and R. Dörner, J. Phys. B: At., Mol. Opt. Phys. **33**, L127 (2000).

[33]H. J. Werner, P. J. Knowles, G. Knizia, F. R. Manby, and M. Schütz, Wiley Interdiscip. Rev.: Comput. Mol. Sci. **2**, 242 (2012).

[34]H.-J. Werner, P. J. Knowles, G. Knizia, F. R. Manby, M. Schütz *et al.*, MOLPRO, version 2012.1, a package of *ab initio* programs, 2012, see http://www.molpro.net.

[35]C. Hampel, K. A. Peterson, and H. J. Werner, Chem. Phys. Lett. **190**, 1 (1992).

[36]M. W. Schmidt, K. K. Baldridge, J. A. Boatz, S. T. Elbert, M. S. Gordon, J. H. Jensen, S. Koseki, N. Matsunaga, K. A. Nguyen, S. Su, T. L. Windus, M. Dupuis, and J. A. Montgomery, Jr, J. Comput. Chem. **14**, 1347 (1993).

[37]P. Piecuch, S. A. Kucharski, K. Kowalski, and M. Musiał, Comput. Phys. Commun. **149**, 71 (2002).

[38]M. Włoch, J. R. Gour, K. Kowalski, and P. Piecuch, J. Chem. Phys. **122**, 214107 (2005).

[39]P. Wang, A. M. Sayler, K. D. Carnes, B. D. Esry, and I. Ben-Itzhak, Opt. Lett. **30**, 664 (2005).

[40]X. Zhu, V. V. Lozovoy, J. D. Shah, and M. Dantus, J. Phys. Chem. A **115**, 1305 (2011).

[41]A. Konar, Y. Shu, V. V. Lozovoy, J. E. Jackson, B. G. Levine, and M. Dantus, J. Phys. Chem. A **118**, 11433 (2014).